Molecular Crystals and Liquid Crystals Science and Technology. Section A. Molecular Crystals and Liquid Crystals

Publication details, including instructions for authors and subscription information:
http://www.tandfonline.com/loi/gmcl19

Pyroelectric Investigations on a Ferroelectric Side-Chain Polysiloxane Using the Laser Intensity Modulation Method (Limm)

N. Leister [a] , D. Geschke [a] & M. V. Kozlovsky [b]

[a] University of Leipzig, Faculty of Physics and Geosciences, Department of Polymer Physics, Linnéstrasse 5, 04103, Leipzig, Germany

[b] Technical University Darmstadt, Institute of Physical Chemistry, Petersenstrasse 20, 64287, Darmstadt, Germany

Version of record first published: 04 Oct 2006

To cite this article: N. Leister, D. Geschke & M. V. Kozlovsky (1998): Pyroelectric Investigations on a Ferroelectric Side-Chain Polysiloxane Using the Laser Intensity Modulation Method (Limm), Molecular Crystals and Liquid Crystals Science and Technology. Section A. Molecular Crystals and Liquid Crystals, 309:1, 201-216

To link to this article: http://dx.doi.org/10.1080/10587259808045529

Mol. Cryst. Liq. Cryst., 1998, Vol. 309, pp. 201–216
Reprints available directly from the publisher
Photocopying permitted by license only

Pyroelectric Investigations on a Ferroelectric Side-Chain Polysiloxane Using the Laser Intensity Modulation Method (LIMM)

N. LEISTER[a], D. GESCHKE[a] and M. V. KOZLOVSKY[b]

[a]*University of Leipzig, Faculty of Physics and Geosciences, Department of Polymer Physics, Linnéstrasse 5, 04103 Leipzig, Germany;*
[b]*Technical University Darmstadt, Institute of Physical Chemistry, Petersenstrasse 20, 64287 Darmstadt, Germany*

(Received 11 May 1997; In final form 14 June 1997)

The laser intensity modulation method (LIMM), a pyroelectric technique for investigating spatially resolved polarization and charge distributions has been applied to sandwich cells containing the ferroelectric liquid crystal side-chain polysiloxane P8*S. Nonuniform polarization distributions in samples with a thickness of the LCP layer larger than the helical pitch were investigated. Maxima of opposite sign at the boundaries caused by symmetrical surface anchoring of the molecules were found. Application of a static external electric field allows the investigation of helix unwinding and screening effects due to impurities in the LC. In the latter case charge layers contribute to the distribution. Variation of the sample temperature causes not only a change in response values due to the temperature dependence of the pyroelectric coefficient but also changes the shape of the measured pyrospectrum. The resulting changes in the polarization distribution may be caused by the temperature variation of the pitch.

Keywords: Ferroelectric liquid crystal polymer; spontaneous polarization; pyroelectric measurements; LIMM; surface anchoring

1. INTRODUCTION

The laser intensity modulation method (LIMM) has been developed by Lang [1] for the investigation of spatially resolved polarization and charge distributions. The focus of interest concerning LIMM measurements has been in the field of electret materials like polytetrafluoroethylene FEP (see

for example [2, 3]) or the ferroelectric polyvinylidenefluoride PVDF (see for example [1, 4]) and its copolymer with trifluoroethylene P(VDF-TrFE) (see for example [5]). Effects on resulting distributions due to the modification of material parameters and poling conditions were examined.

Ferroelectric liquid crystalline polymers (FLCP) also gained much interest in recent years because of their possible application in displays or pyroelectric sensors. The spontaneous polarization is one of the physical parameters which characterizes the FLCP material. In the SmC* phase it exists in a single smectic layer but vanishes in the bulk due to a helical structure. The helix has to be unwound either by surface effects or by external fields in order to get a nonvanishing polarization.

In very thin ($1-2\,\mu m$) surface stabilized samples [6] a uniform value of polarization over the cell thickness is caused by surface anchoring of the molecules. The application of an electric field leads to switching between two possible states. In thick samples surface effects can be neglected. Application of a weak field leads to a partial unwinding of the helix. For higher field strength uniform orientation is reached. In samples, which are already thin but have a thickness larger than the helical pitch, a combination of effects takes place. Surface anchoring at the boundaries, a helical structure inside the cell and the existence of disclination lines in between both regions influence the orientation in the sample (see for example [7]). The result of application of an external field becomes more complex. In addition to the helix unwinding disclination lines must vanish in order to give a uniform orientation.

Surface stabilized cells have been in focus of attention with respect to applications. On the other hand grey levels in displays can be realized much easier by means of thicker cells (DHF-display [8]).

There are two standard measurement techniques for the determination of spontaneous polarization P_s. In the first case, a surface stabilized cell is switched from one state to the other (change of polarization sign) and the polarization reversal current is measured [9]. In the second case pyroelectric measurements are performed, which in contrast to LIMM only determine an integrated value of P_s over the cell thickness [10]. For some measurements the determined values have been found dependent on cell thickness [11], which indicates that deviations from the assumed uniform polarization distribution take place.

In addition to these methods LIMM measurements on FLCP cells allow the examination of nonuniform polarization distributions. Surface as well as bulk contributions to the resulting state in dependence on specific properties of cell and substance can be observed. On the one hand this is of fundamental interest in understanding the behaviour of FLCP cells, on the

other hand potential error sources for standard polarization measurements might be found. In the following text measurements with LIMM on a side-chain liquid crystal polysiloxane are presented.

2. EXPERIMENTAL

2.1. Method

The method LIMM is only briefly presented here. Details can be found elsewhere [1, 12]. A sample with a thin metal layer on its surface is irradiated by an intensity modulated laser beam. The metal layer acts simultaneously as light absorber and electrode. A heat wave is generated by light absorption and penetrates into the sample. The penetration depth of the heat wave depends on the modulation frequency. For small frequencies the whole sample is heated almost homogeneously, for high frequencies the heated range is concentrated near the irradiated surface. Variation of the modulation frequency allows a thermal scan of the sample. Charges and dipoles inside the sample react to heating. This causes a pyroelectric current on the electrodes, which is measured.

The following equation [12] gives the pyroelectric current I_p for fixed modulation frequency ω:

$$I_p(\omega) = \frac{A}{L}\int_0^L r(z)\frac{\partial T(\omega, z)}{\partial t}dz, \quad r(z) = g(z) + (\alpha_\varepsilon - \alpha_z)\varepsilon\varepsilon_0 E(z). \tag{1}$$

A is the electrode area, L the sample thickness. The temperature profile $T(\omega, z)$ at the modulation frequency ω is given by a solution of the heat conduction equation (see for example [12]). $r(z)$ is the distribution searched for. $r(z)$ has contributions from the pyroelectric coefficient $g(z) = dP_s/dT$ and the electric field $E(z)$ caused by charges in the sample. ($\alpha_\varepsilon = 1/\varepsilon\, \partial\varepsilon/\partial T$ is the temperature coefficient of permittivity, $\alpha_z = 1/z\, \partial z/\partial T$ the temperature coefficient of thickness.)

The field $E(z)$ is given by the following equations:

$$\begin{aligned} E(z) &= R(z) - \overline{R}, \quad R(z) = \int_0^z \rho_{\text{ges}}(\zeta)d\zeta, \\ \overline{R} &= \frac{1}{L}\int_0^L R(z)dz, \quad \rho_{\text{ges}} = \rho - \frac{dP_r}{dz}. \end{aligned} \tag{2}$$

If the polarization is locally compensated by charges $\rho = dP_r/dz$, then $E(z) = 0$ holds and, therefore, $r(z)$ has only contributions from the pyrocoefficient $g(z)$.

The distribution $r(z)$ has to be determined by deconvolution from the spectrum of the pyroelectric current $I_p(\omega)$.

The experimental setup used here and the numerical deconvolution by means of the Tikhonov regularisation technique are based on the work of Bloss, Steffen and Schäfer [3, 12, 13, 14].

The experimental setup (Fig. 1), as described by Bloss [12], has been modified concerning the possibility of measurements under external field and the temperature control of the sample. Therefore the setup is described as a whole again: The sample is placed in a mounting, which is shielded in order to avoid external disturbances. The beam of a helium-neon-laser with a nominal output of 25 mW, intensity-modulated sinusoidally by an acoustooptic modulator (AOM), is incident on the upper metal layer, while the rear side of the sample is thermally contacted to a heat sink. The pyroelectric current is detected and converted to a voltage by a current-to-voltage-converter (CVC) with amplification factor 1 MV/A. This voltage is detected by a lock-in-amplifier with respect to the phase of the incident light, which results in a signal consisting of real and imaginary part. The AOM is driven by a function generator which also produces the reference frequency for the lock-in-amplifier. Function generator and lock-in-amplifier are controlled by a computer.

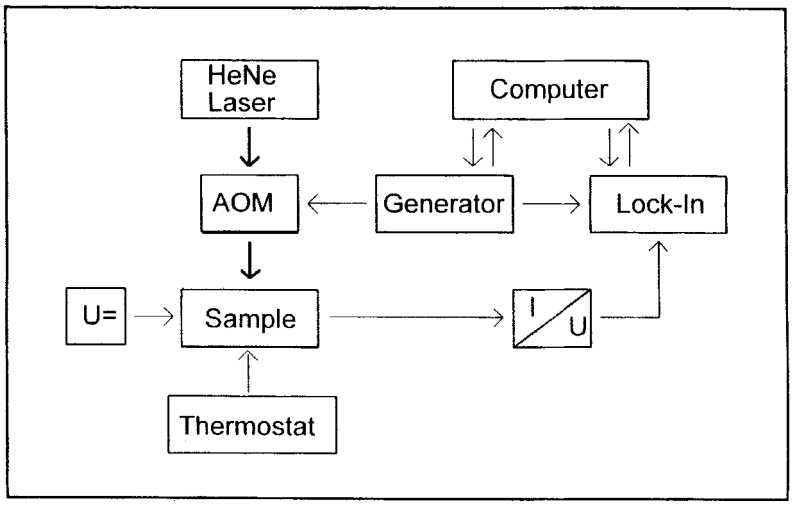

FIGURE 1 Experimental setup for LIMM measurements.

In contrast to former measurements, where stable distributions on externally poled samples were investigated, the possibility was added to apply an external electric field during measurements. A battery driven voltage source (0–180 V) is used in order to minimize noise and to avoid disturbance of the signal. This is necessary because of the measurement of very small currents typically in the range of some picoampere. The voltage source is coupled to the CVC through a capacity.

The temperature control is carried out by heating of the whole sample holder, to which the sample is thermally contacted. The sample holder has a hollow space with water flowing through and is connected to a thermostat. The temperature is controlled by a PT100 element and kept constant during measurement.

2.2. Samples

The material used here is the side-chain liquid crystal polysiloxane P8*S. Synthesis of this polymer has been described previously [15]. The average degree of polymerization is 35. It has a phase sequence g 31–35°C S_C* 43°C S_A* 47°C I in thin films. The chemical structure is shown in Figure 2.

A cell similar to that described by Steffen [14] is used. The LCP is placed in a sandwich cell, front and rear sides consisting of Kapton® polyimid foil (PI), thickness 7.5 μm. The cover foils were vacuum deposited with a gold and bismuth layer (bismuth has higher absorptivity than gold [16]). These electrodes are of circular shape with a diameter of 2 mm, which corresponds to the size of the laser beam. In one sample Mylar® foil (thickness 2.5 μm) is used instead of Kapton®.

The LCP is filled into the sample cell in its isotropic phase at about 70°C and then slowly cooled down. It is then exposed to repeated heating and

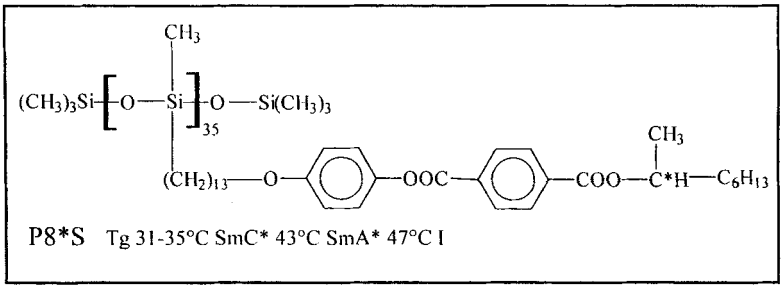

FIGURE 2 Chemical structure of the polymer P8*S.

cooling cycles near the phase transition (S_C^* to S_A^*) for some time. Polarization microscopy shows a stripe shaped texture.

3. RESULTS AND DISCUSSION

3.1. Measurements without External Field at Room Temperature

Samples with LCP layers which are thin enough that surface interaction is of importance but thick enough to have a nonuniform polarization distribution were prepared. The thickness of the LCP layer was in the range from 6 to 15 μm. The influence of the surface interaction on the polarization distribution in these samples was investigated by measurements without an external field.

Figure 3a shows a typical pyroelectric spectrum for a sample of a total thickness of 28 μm (13 μm LCP layer). In order to be sure that signals are caused by polarization of the LCP, test measurements for samples without an LCP layer were carried out. No response could be found, neither from the polyimid foil itself, nor from a cell filled up by dielectric silicon grease. Furthermore for the LCP samples the signal vanished when the temperature was above the phase transition $S_C^* - S_A^*$.

As compared to former measurements on a nematic LCP, where a frozen in polarization distribution was obtained by thermal poling [14], the signal for P8*S is about 20 times larger. This is partly due to material and to different cell setup as well (bismuth layer with higher absorbtivity). The improvement in signal-to-noise-ratio makes deconvolution results more reliable. No absolute values were determined here, the distributions are given in arbitrary units. Values for the pyroelectric coefficient of this material have been reported elsewhere [17]. They are in the range between 0.3 nC/cm^2K at 25°C and 1.2 nC/cm^2K at 40°C.

The deconvolution procedure using Tikhonov regularisation is described elsewhere [12]. Knowledge of the temperature profile $T(\omega, z)$ is needed to obtain $r(z)$ as can be seen in equation 1. $T(\omega, z)$ depends on material parameters, the thermal conductivity and the thermal diffusivity of the LCP, and on the heat transfer coefficient on the rear side of the sample, resulting from experimental setup. These parameters are unknown but can be determined in an iterative procedure, where the residues of the regularization are minimized [13]. Similar values for the LCP and the PI foil are assumed and the solution of the heat conduction equation for one uniform layer is used, as discussed previously [14]. Thus average values are

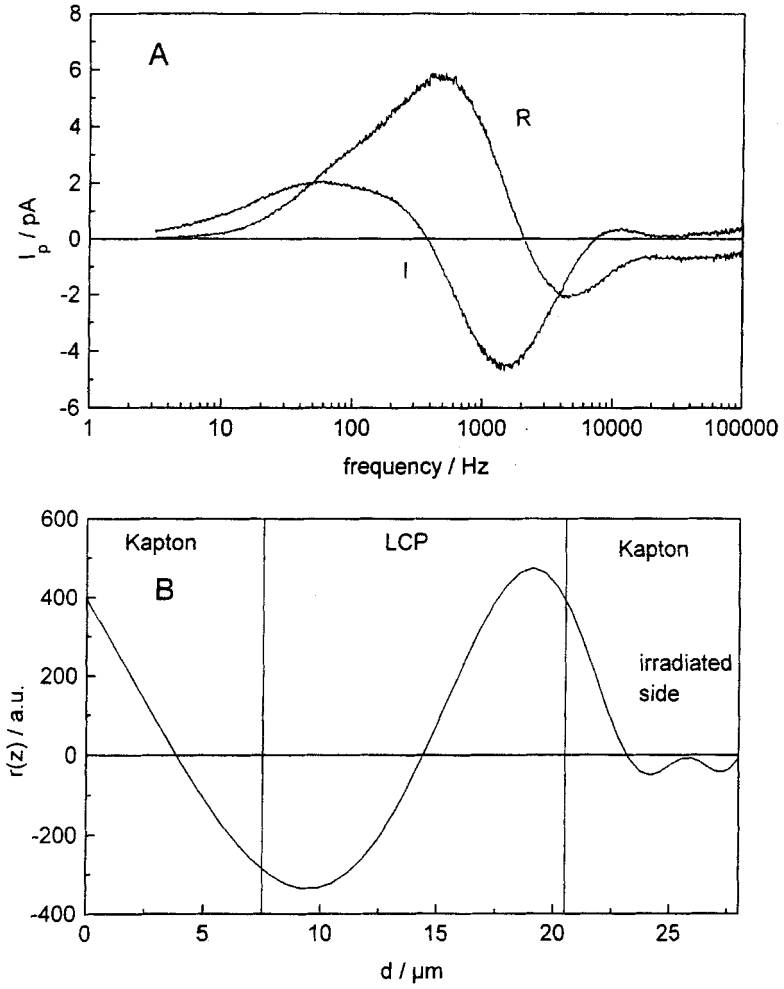

FIGURE 3 P8*S, cell with 13 μm LCP layer and 7.5 μm Kapton® foil at 25°C a) pyroelectric current (R = real part, I = imaginary part), b) distribution $r(z)$.

determined. The result for diffusivity varies between 8.7 and 9.5 m^2/s for different samples. Taking into consideration the known value for Kapton (7.7 m^2/s) [18] and the cell thickness, a diffusivity of about 11.5 m^2/s for the LCP can be estimated. For thermal conductivity a value of 0.15 J/(smK) is assumed. The heat transfer coefficient shows typical values, which have also been found in former investigations. As the LCP is a polysiloxane, data from literature for polydimethylsiloxane are given for comparison. Values

for thermal conductivity κ differ between 0.13 J/smK [19] and 0.22 J/smK [20]. With the heat capacity c_p (1.47 J/gK [19] or 1.59 J/gK [19,20]) and the density $\rho = 0.98$ g/cm^3 [19] a diffusivity $\chi = \kappa / (c_p \rho)$ can be calculated ranging from 8.3 to 14.3 m^2/s. The value for the LCP obtained by iteration is in the middle of this range.

The distribution resulting from the spectrum in Figure 3a is shown in Figure 3b. Maxima of different sign can be seen at both boundaries. The positive value inside the polyimid layer on the rear side is caused by numerical deviations, similar to previous results [14].

In the SmC* phase the spontaneous polarization of a single layer vanishes in the bulk due to a helical structure. In a sample with a thickness larger than the pitch the inner parts of the LCP layer should give no resulting polarization while at the surface nonzero polarization is expected because of surface anchoring. For parallel orientation of the mesogenic units, the polarization vector is perpendicular to the surface. (The existence of a pretilt would lead to a polarization not being perpendicular and therefore to a smaller value of the pyrosignal, because only one component of the polarization vector is detected.) Symmetrical anchoring, which means that polarization vector is pointing either outward at both surfaces or inward at both surfaces, causes different sign of the detected component at both boundaries. This is in agreement with the experimental results. On the other hand a broader range of zero polarization in the middle part of the LCP layer, which would be expected, can not be seen here.

The absence of that zero part may be due to decrease in resolution of the method with rising penetration depth. The use of 7.5 μm Kapton® foil leads to total sample thickness of 28 μm. For comparison a sandwich cell of 6 μm LCP layer between 2.5 μm Mylar® foil has been investigated (total thickness 11 μm). The pyrosignal is shifted to higher frequencies and also improved in magnitude because of the reduced foil thickness. The distribution (Fig. 4) has maxima at the surfaces which are much narrower and contains an area inside the sample with the value 0. Differences in distribution may also be caused by different surface interactions of the LCP with Kapton® and Mylar® but better resolution is a more likely explanation for the observed effects. Until now only a few samples using Mylar® foil have been investigated. All further results presented here are from samples with Kapton® foil.

While both samples mentioned above have distributions with maxima of approximately equal size at both boundaries, for other samples the relative size differs. In order to confirm this fact and to exclude systematic errors due to the deconvolution procedure, a sample has been turned round and has

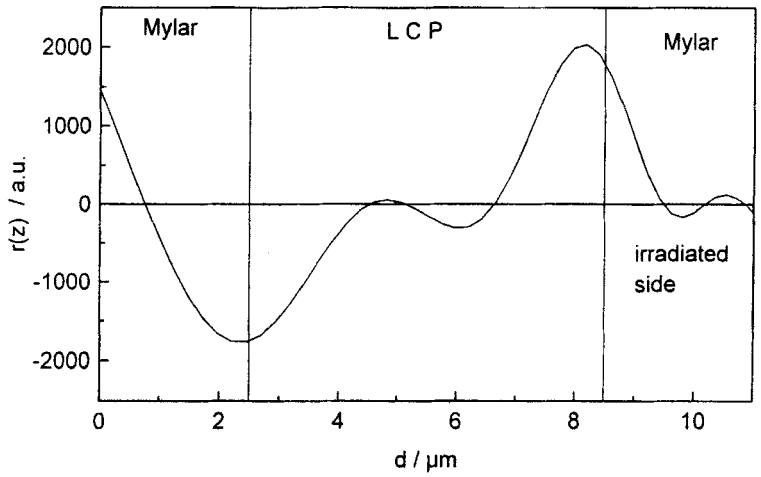

FIGURE 4 P8*S, cell with 6 µm LCP layer and 2.5 µm Mylar® foil at 25°C, distribution $r(z)$.

been irradiated from the other side. A comparison of the results obtained from both measurements shows good agreement except from numerical deviations near the rear surface. An explanation for the different magnitude of the maxima is still lacking.

3.2. Measurements with External Field at Room Temperature

The influence of an external electric field on the polarization distribution was examined. A transition from a nonuniform distribution caused by surface anchoring to a uniform one due to orientation of the molecules by the field was expected to take place with rising field strength.

The observed effects were different: The maximum change in the pyrospectra took place at high frequencies (> 1 kHz). Those frequencies correspond to penetration depths where the heat wave remains inside the polyimid and does not reach the LCP layer. Deconvolution results showed no change inside the LCP layer. The contribution to $r(z)$ due to surface anchoring remained almost the same, whereas an additional contribution inside the polyimid foil gets larger with rising voltage. As polyimid itself is not pyroelectric polarization effects inside the PI layer can be excluded. The sample behaviour can be explained by screening effects due to impurities inside the LCP, which move to the surface under the influence of an external field [21]. The charges on the surfaces of the polyimid foil cause an electric

field inside the foil, which contributes to $r(z)$ (see equation 1). This effect will be discussed in more detail in a future publication.

3.3. Temperature Variation

Samples were temperature controlled in order to make measurements in the range between 30 and 45°C. This was done for the following two reasons:

- The sample is below its glass transition at room temperature. This may beside screening also contribute to the fact that a change in polarization due to an external field was not seen at this temperature. For higher temperature values the situation was expected to be different.
- A change in the pyrosignal above the phase transition S_C^* to S_A^* was expected. This should be an additional verification that the results described above are really due to ferroelectric polarization.

Both effects were found. In addition an unexpected change in the shape of the pyrosignal and the resulting distribution in the range of 36–38°C compared to the measurements at 25°C took place.

Figure 5a gives the real part of pyroelectric spectra for measurements on the same sample at 25°C and at 38°C without external field. The change in magnitude of the signal might be due to temperature variation of the pyrocoefficient $g(z)$. Also a change in signal shape is obvious. The maximum is shifted to lower frequencies. The distribution has the usual maxima at the boundaries at 25°C and changes to an almost uniform one at 38°C (Fig. 5b).

Distributions for a different sample are shown in Figures 6a, 6b, 6c. The following effects can be seen:

- The variation of signal magnitude with temperature is different as compared to the first sample. In Figure 6a (without field) there is a rise up to 32°C, then the signal decreases again.
- The changes in signal shape are similar to the first sample: In Figure 6a the maximum is concentrated near the surface at first, then it gets more uniform over the whole LCP layer for higher temperatures. The measurement at 38°C could not be deconvoluted satisfactorily, but the measured signal shape seems to continue this trend. For measurements with field (Figs. 6b, 6c) the behaviour of the signal shape is qualitatively the same as without field apart from the fact, that additional contributions inside the polyimid layer due to charges arise.
- Comparing measurements at fixed temperatures in Figures 6a, 6b and 6c it can be seen that for 36°C and 38°C there is a rise in signal magnitude

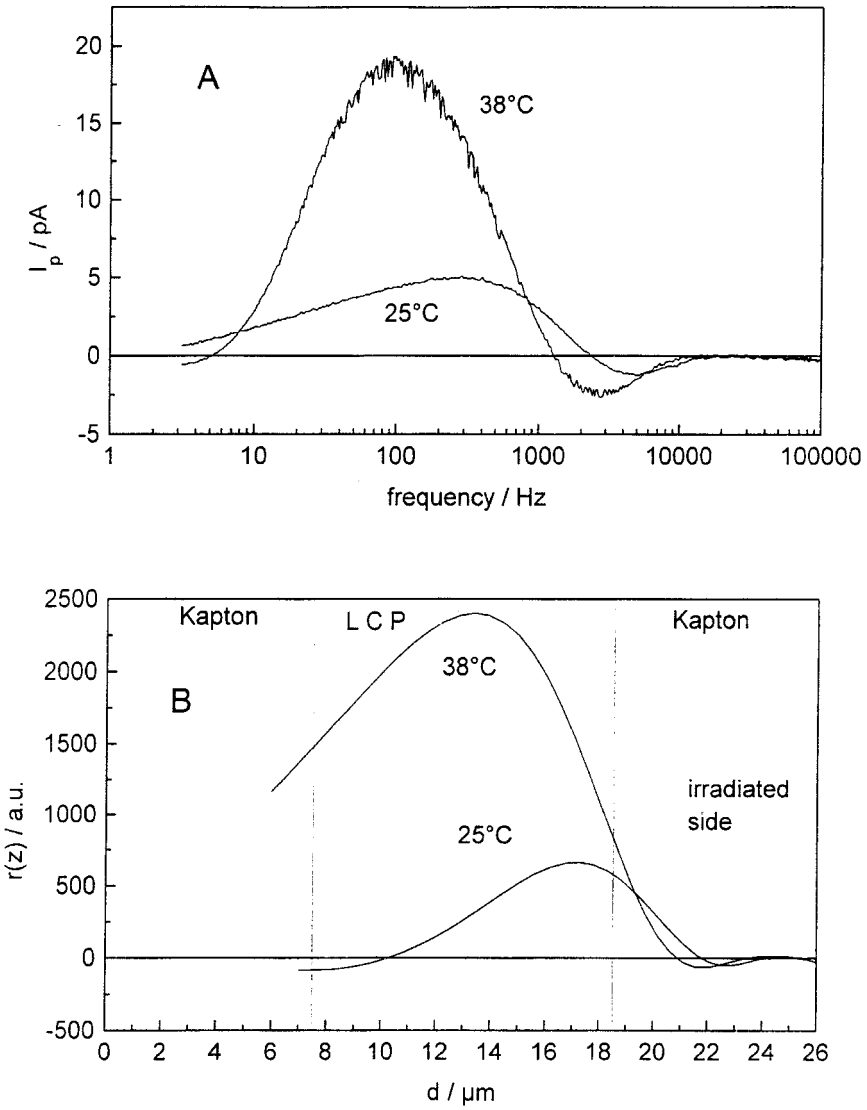

FIGURE 5 Temperature dependence: P8*S, cell with 11 μm LCP layer and 7.5 μm Kapton® foil, measurements at 25°C and 38°C. a) real part of pyroelectric current at 25°C and at 38°C, b) corresponding distributions $r(z)$.

with applied voltage. Contributions from inside the polyimid layer caused by charges and those caused by polarization can not be separated because of limited resolution, but clearly a rise can be seen inside the LCP layer. So in this temperature range, the LCP does react on the field despite of

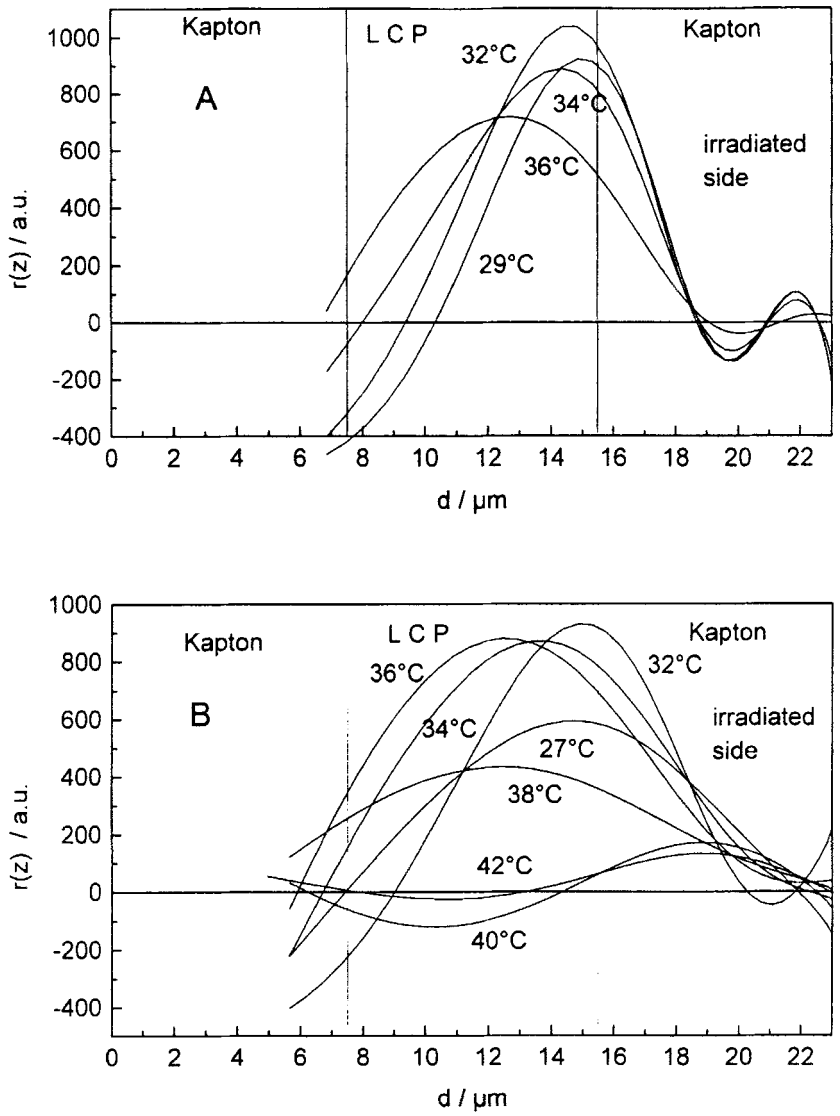

FIGURE 6 Temperature dependence, different sample: P8*S, cell with 8 µm LCP layer and 7.5 µm Kapton® foil. a) distributions $r(z)$ for measurements without applied voltage, b) distributions $r(z)$ for measurements at U = 54 volt, c) distributions $r(z)$ for measurements at U = 108 volt.

partial screening. The applied voltage is not high enough to get saturation. In previous investigations on this material [17] low saturation fields of 1.5 V/µm were found with a commercial EHC cell and 0.5 V/µm

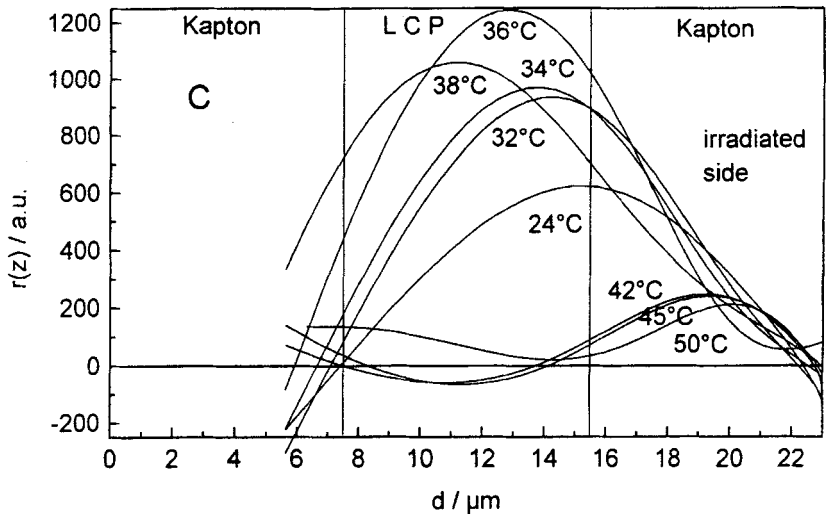

FIGURE 6 (Continued).

for a self made cell (lower than typical saturation values for FLC polymers). Clearly the screening effects depend on the thickness of the polymer layer in usual cells and the thickness of the polymer foil for the samples used here, respectively.

- A further characteristic change in signal shape takes place at a temperature of about 40°C. The distribution is then concentrated inside the polyimid foil while the contribution from the LCP layer vanishes. At further heating the signal does not change with temperature any more. It should be reminded, that this part of the signal is caused by screening charges alone and that no remaining polarization is left in this temperature range. From DSC data [17] a phase transition S_C^* to S_A^* was detected at 43–44°C, which slightly differs from the results given here, but is in qualitative agreement.

A change in the shape of the pyrospectrum may have two reasons as shown in equation 1: the change of $r(z)$ or change of $T(\omega, z)$. It has to be confirmed that the observed effects are really due to a change in polarization distribution.

The temperature distribution at a fixed modulation frequency $T(\omega, z)$ is influenced by thermal parameters of the sample. An appreciable change of thermal diffusivity near the phase transition would lead to different

pyrospectra. The usual way of determining thermal parameters iteratively was not applicable here. As varying temperature and voltage makes necessary a large number of measurements, which is very time consuming, the number of data points was reduced. At room temperature a measurement with normal resolution (451 data points) was made and used for the iteration procedure. At higher temperatures only 91 data points were taken. The room temperature parameter set was used for deconvolution. Small residues were found in the deconvolution process, but the limited number of data points may cover systematic deviations.

On the other hand errors caused by deconvolution with wrong thermal parameters can be excluded, if two measurements with irradiation of the sample from both sides are made. Wrong values of thermal diffusivity lead to broadening or narrowing of the distribution. This would cause corresponding distributions to be in disagreement in the middle part. No disagreement was found in this investigations.

Therefore the results should be considered as actually due to changes in the polarization distribution with the temperature. A possible explanation for this change is suggested: The value for the pitch at room temperature has been determined to be 3.3 μm [17]. The usual temperature behaviour of the pitch in a ferroelectric LC shows a significant rise near the phase transition point (see for example [22]). For a sample with a LCP layer thickness of only 8 μm, which is about two and a half the value of the pitch at room temperature, these changes may have significant effects on the molecular orientation inside the sample.

It should be mentioned that such a behaviour may lead to errors when the temperature dependence of the polarization is investigated by standard methods, which determine only an integral value.

An explanation for the different temperature variation of the signal magnitude for individual samples is still lacking. In case of a uniform polarization distribution the value of polarization changes with the temperature and a corresponding change of the pyrocoefficient $g = dP_s/dT$ may cause a different magnitude of the pyrosignal. For nonuniform distributions the different relative magnitude of the maxima at both boundaries for individual samples and its influence on the temperature behaviour has to be taken into account additionally. At higher temperatures the smaller of the two maxima vanishes but the magnitude of the resulting distribution may depend on the initial state. Further investigations concerning these phenomena are under progress.

4. CONCLUSIONS

Spatially resolved polarization and charge profiles in a ferroelectric liquid crystal side-chain polysiloxane have been determined by the LIMM technique.

Nonuniform polarization distributions in samples with a thickness larger than the helical pitch have been found. These distributions show maxima of different sign at the boundaries, a fact that can be explained by symmetrical surface anchoring. When an external electric field is applied screening effects have been observed, which are caused by impurities in the material. No effect of the field on the LCP layer has been observed at room temperature below the glass transition point. A rise in signal magnitude due to the orientation of molecules by field can be seen in the range 36–38°C. Temperature variation leads to changes in the shape of the polarization distribution. A possible explanation could be the temperature variation of the pitch and its influence on the molecular orientation in the sample. The use of a different cell with Mylar® foil allows a better spatial resolution. This will help to make further improvement in future investigations.

Acknowledgements

Financial support by the Deutsche Forschungsgemeinschaft within the research project No. Ge 718/4-1 is gratefully acknowledged.

References

[1] S. B. Lang and D. K. Das-Gupta, *J. Appl. Phys.*, **59**, 2151 (1986).
[2] D. K. Das-Gupta, J. S. Hornsby, G. M. Yang and G. M. Sessler, *J. Phys. D: Appl. Phys.*, **29**, 3113 (1996).
[3] P. Bloss, M. Steffen H. Schäfer, G. M. Yang and G. M. Sessler, *IEEE Trans. Dielectr. Electr. Insul.*, **3**, 182 (1996).
[4] P. Bloss, M. Steffen, H. Schäfer, G. Eberle and W. Eisenmenger, *IEEE Trans. Dielectr. Electr. Insul.*, **3**, 417 (1996).
[5] B. Ploss and O. Bianzano, *Proceedings of the 8th International Symposium on Electrets*, 206 (1994).
[6] N. A. Clark and S. T. Lagerwall, *Appl. Phys. Lett.*, **36**, 899 (1980).
[7] M. Brunet and P. Martinot-Lagarde, *J. Phys. II France*, **6**, 1687 (1996).
[8] J. Fuenfschilling and M. Schadt, *Jpn. J. Appl. Phys.*, **35**, 5765 (1996).
[9] P. Martinot-Lagarde, *J. Phys. (Paris)*, **38**, L17 (1977).
[10] L. H. Yu, H. Lee, C. S. Bak and M. M. Labes, *Phys. Rev. Lett.*, **36**, 388 (1976).
[11] A. Kocot, R. Wrzalik, J. K. Vij and R. Zentel, *J. Appl. Phys.*, **75**, 728 (1994).
[12] P. Bloss and H. Schäfer, *Rev. Sci. Instr.*, **65**, 1541 (1994).
[13] M. Steffen, P. Bloss and H. Schäfer, *Proceedings of the 8th International Symposium on Electrets*, 200 (1994).
[14] M. Steffen, P. Bloss, H. Schäfer, M. Winkler and D. Geschke, *Liq. Cryst.*, **19**, 93 (1995).
[15] M. V. Kozlovsky and E. I. Demikhov, *Mol. Cryst. Liq. Cryst.*, **282**, 11 (1996).

[16] S. Bauer and B. Ploss, *J. Appl. Phys.*, **68**, 6361 (1990).
[17] M. V. Kozlovsky, M. Darius and W. Haase, *ECLC'97, European Conference on Liquid Crystals*, Zakopane, Poland, March 1997.
[18] Dupont data sheet.
[19] W. van Krevelen, *Properties of Polymers* (Elsevier, Amsterdam, 1990).
[20] J. E. Mark, *Physical Properties of Polymers Handbook* (Woodbury, New York, 1996).
[21] K. H. Yang, T. C. Chieu and S. Osofsky, *Appl. Phys. Lett.*, **55**, 125 (1989).
[22] L. M. Blinov and V. G. Chigrinov, *Electrooptic effects in Liquid Crystal Materials*, (Springer, Berlin), 380.